ANALYSIS OF AN ELEMENTARY REACTION MECHANISM FOR BENZENE OXIDATION IN SUPERCRITICAL WATER

JOANNA L. DINARO,[1] JACK B. HOWARD,[1] WILLIAM H. GREEN,[1] JEFFERSON W. TESTER[1]
AND JOSEPH W. BOZZELLI[2]

[1]Department of Chemical Engineering and Energy Laboratory
Massachusetts Institute of Technology
Cambridge, MA 02139, USA
[2]Chemistry and Chemical Engineering Department
New Jersey Institute of Technology
Newark, NJ 07102, USA

A benzene supercritical water oxidation (SCWO) mechanism, based on published low-pressure benzene combustion mechanisms and submechanisms describing the oxidation of key intermediates, was developed and analyzed to determine the controlling reactions under SCWO conditions of 750–860 K, 139–278 bar, and equivalence ratios from 0.5 to 2.5. To adapt the combustion mechanisms to the lower temperature (<975 K) and higher pressure (>220 bar) conditions, new reaction pathways were added, and quantum Rice–Ramsperger–Kassel theory was used to calculate the rate coefficients and, hence, product selectivities for pressure-dependent reactions. The most important difference between the benzene oxidation mechanism for supercritical water conditions and those for combustion conditions is reactions in supercritical water involving C_6H_5OO predicted to be formed by C_6H_5 reacting with O_2. Through the adjustment of the rate coefficients of two thermal decomposition pathways of C_6H_5OO, whose values are unknown, the model accurately predicts the measured benzene and phenol concentration profiles at 813 K, 246 bar, stoichiometric oxygen, and 3–7 s residence time and reproduces the finding that the carbon dioxide concentration exceeds that of carbon monoxide at all reaction conditions and levels of benzene conversion. Comparison of the model predictions to benzene SCWO data measured at several different conditions reveals that the model qualitatively explains the trends of the data and gives good quantitative agreement without further adjustment of rate coefficients.

Introduction

Supercritical water oxidation (SCWO) is a remediation process for treating aqueous organic wastes. When organic compounds and oxygen are brought together in water well above its critical point of 221 bar and 647 K, the organic is oxidized to carbon dioxide and water, heteroatoms are converted to their corresponding mineral acids and can be neutralized using a suitable base, and any nitrogen forms N_2 or N_2O [1]. The present working hypothesis maintains that SCWO proceeds by free-radical reactions and that the individual elementary reactions are similar to those which would take place in combustion at the temperature and pressure of SCWO. Furthermore, water, which serves as the reaction medium and participates in reactions both as a reactant and as a third-body collider, does not interfere with reaction events through solvation effects.

The free-radical reaction pathway hypothesis has received support by multiple attempts to model reactions using low-pressure combustion mechanisms adapted to SCWO conditions. Previous modeling efforts yielded kinetic mechanisms describing the oxidation of simple compounds such as hydrogen [2–7], carbon monoxide [3,5,6], methane [5,6,8,9], methanol [6,7,10–14], and phenol [15]. The model predictions have been compared, with varying degrees of success, to experimentally measured species concentration profiles.

An elementary reaction mechanism for benzene oxidation under supercritical water conditions was developed [16] based on a detailed kinetic mechanism for benzene oxidation under combustion conditions [17,18]. The present paper reports results obtained using this developed mechanism to identify reactions controlling benzene oxidation under supercritical water conditions. The model predictions are compared with benzene and phenol concentration profiles measured in our experimental investigation of benzene SCWO at 750–860 K and sub- to supercritical pressures (139–278 bar) under fuel-rich to fuel-lean conditions for reactor residence times of 3–7 s [19]. The details of these experiments are reported elsewhere [19], but briefly benzene SCWO was studied in an 11 mL Hastelloy C276 tubular plug-flow reactor. Temperature was controlled by immersing the reactor in a fluidized sand bath. Aqueous feed solutions of benzene and oxidant were

pressurized, preheated, and delivered to the reactor. The reactor effluent was immediately quenched and analyzed for unreacted benzene and oxidation products. Upwards of 90% of the reacted benzene was accounted for in phenol, carbon monoxide, carbon dioxide, and methane.

The various mechanisms developed to model benzene combustion successfully predict the oxidation of benzene as well as many other stable and radical intermediates [17,18,20–24]. The main shortcomings of these models are their pronounced overpredictions of the concentrations of C_6H_5, C_6H_5O, and C_6H_5OH. Given that these species are the primary products of benzene oxidation, this inaccuracy is troubling. As noted by Chai and Pfefferle [25], the current benzene oxidation models, developed primarily for temperatures above 1600 K and fuel-rich conditions, are not usable outside of the temperature and stoichiometric conditions for which they were adjusted, and the understanding of the detailed oxidation mechanism is particularly poor at 900–1300 K and fuel-lean conditions. Under SCWO conditions, new reaction pathways may be accessible due to the higher pressure, and thermal decomposition pathways with high activation barriers which play important roles at combustion conditions may be inaccessible due to the lower temperatures. Therefore, comparisons of the predictions of a current benzene combustion mechanism [17,18] against our data for the SCWO of benzene will test the robustness of the mechanism while furthering the understanding of benzene oxidation.

Adaptation of Benzene Oxidation Mechanisms from Combustion to Supercritical Water Conditions

The most obvious modification necessary to make low-pressure combustion mechanisms suitable for SCWO conditions is adjustment of reaction rate coefficients for the effect of pressure. Unimolecular rate coefficients are well known to depend on pressure to a power which is unity in the low-pressure limit, zero in the high-pressure limit, and fractional in the intermediate-pressure or fall-off region. The transitions to the low- and high-pressure limits occur at reaction-specific pressures.

Recombination reactions exhibit the same pressure dependence as unimolecular reactions when only one reaction pathway is possible. When additional products can be formed by chemically activated pathways, a complex pressure and temperature dependence can result from the competition between the stabilization and the decomposition and/or isomerization pathways [26,27], and experimentally measured rate coefficients cannot be extrapolated directly to other temperatures and pressures. The computer programs CHEMACT [27] and

CHEMDIS [28,29] implement the bimolecular Quantum Rice Ramsperger Kassel (QRRK) analysis of Dean [26] and allow the estimation of the pressure and temperature dependence of the rate coefficients for such reactions. Westmoreland et al. [30] and Dean [26] discussed the governing bimolecular and unimolecular QRRK equations and compared predicted and measured rate coefficients. In the present study, two important chemically activated reactions, between H and O_2 and between phenyl (C_6H_5) and O_2, were evaluated.

$H + O_2 \leftrightarrow HO_2^* \leftrightarrow OH + O$

The addition/elimination reaction between H and O_2 is one of the most important chain-branching steps in low-pressure combustion. The addition/elimination pathway proceeds through the formation of the activated intermediate HO_2^*, which can be stabilized to HO_2 or dissociate to OH and O. The relative importance of the two pathways depends on pressure and temperature, with the HO_2-forming pathway favored at higher pressures.

Cobos et al. [31] studied the recombination reaction forming HO_2 at 298 K and 1–200 bar and estimated the high-pressure rate coefficient for recombination by extrapolating measured fall-off curves. Westmoreland et al. [30] used this high-pressure rate coefficient in a bimolecular QRRK analysis of the reaction between H and O_2. The rates of both the stabilization (to HO_2) and addition/elimination (to OH and O) pathways were successfully predicted over wide ranges of temperature and pressure.

A bimolecular QRRK analysis similar to that of Westmoreland et al., conducted using CHEMACT with rate coefficients from Cobos et al. [31] and Baulch et al. [32], predicted HO_2 to be the primary product of the reaction between H and O_2 at 246 bar and 813 K (for which conditions the most complete set of benzene concentration data are available [19]) with a rate coefficient close to the high-pressure limit [31]. Further calculations reveal excellent agreement between the predicted and measured rate coefficients for the recombination reaction in the high- [31] and low-pressure limit [32] and the addition/elimination pathway [32].
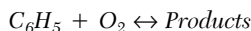
$C_6H_5 + O_2 \leftrightarrow Products$

The identity and formation rate of products of the reaction between phenyl and oxygen are a focus of continuing study. In previous benzene oxidation mechanisms, the products were set to phenoxy (C_6H_5O) and O [17,18,20–23]. A semiglobal pathway was also included in some of these mechanisms [17,18,23]:

$$C_6H_5 + O_2 \leftrightarrow 2CO + C_2H_2 + C_2H_3 \quad (R1)$$

Frank et al. [33] studied the reaction of phenyl with O_2 between 900 and 1800 K and 1.3 to 2.5 bar

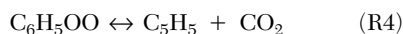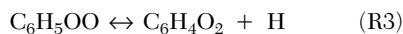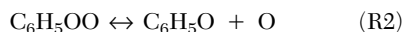| T(K)	Measured by Frank et al. [33]	Predicted by QRRK
1000	1.2×10^{12}	1.6×10^{12}
1100	1.6×10^{12}	2.0×10^{12}
1200	2.0×10^{12}	2.2×10^{12}

and proposed two sets of products: (1) C_6H_5O and O and (2) p-benzoquinone ($C_6H_4O_2$) and H. The second of these overall addition/elimination pathways was necessary to explain their observation of fast initial H production. Rate coefficients were measured for both pathways and were included in a mechanism by Tan and Frank [24].

Yu and Lin [34] performed a direct study on the reaction between C_6H_5 and O_2 at 297–500 K and 20–80 Torr. The overall reactions leading to C_6H_5O and O or $C_6H_4O_2$ and H proceed first through the formation of an energized C_6H_5OO radical ($C_6H_5OO^*$), which can undergo stabilization, isomerization, and/or dissociation to new products. Yu and Lin measured the recombination rate coefficient for $C_6H_5 + O_2$ by monitoring C_6H_5OO formation and found it to be pressure independent under their conditions. The sole reaction product was C_6H_5OO, consistent with their Rice–Ramsperger–Kassel–Marcus prediction that stabilization to C_6H_5OO dominates over addition/elimination to C_6H_5O and O or $C_6H_4O_2$ and H below 1000 K and between 20 and 80 Torr.

Since the reaction between C_6H_5 and O_2 proceeds through the formation of $C_6H_5OO^*$, the rate coefficients for the addition/elimination pathways measured at the conditions of Frank et al. [33] or used in low-pressure mechanisms [17,18,20–24] are not applicable at SCWO conditions. CHEMDIS was used to calculate the rate coefficients for stabilization (to C_6H_5OO) and addition/elimination (to C_6H_5O and O). The high-pressure rate coefficient for C_6H_5OO formation was taken from Yu and Lin [34], and the high-pressure rate coefficient for dissociation of $C_6H_5OO^*$ to C_6H_5O and O was estimated from microscopic reversibility and assuming the reverse reaction has a pre-exponential factor for diffusion-controlled reactions ($A = 10^{12}$ cm^3 mol^{-1} s^{-1}) and no energy barrier ($E_a = 0$). At 813 K and 246 bar, the calculated stabilization rate coefficient is two orders of magnitude larger than that for addition/elimination to C_6H_5O and O. A comparison between the predicted and measured [33] rate coefficients for the addition/elimination pathway at 2.3 bar and from 1000 to 1200 K showed agreement to

within 10% to 20% (Table 1), indicating that the estimated value of k_∞ for $C_6H_5OO^*$ dissociation to C_6H_5O and O may not be a source of significant error.

Since C_6H_5OO was predicted to be the main reaction product of C_6H_5 and O_2, bimolecular and unimolecular reactions of C_6H_5OO were also incorporated into the benzene SCWO mechanism [16]. The rates of the unimolecular reaction were found to dominate at supercritical water conditions. The unimolecular decomposition reactions of C_6H_5OO tested in the SCWO mechanism are

$$C_6H_5OO \leftrightarrow C_6H_5O + O \qquad \text{(R2)}$$

$$C_6H_5OO \leftrightarrow C_6H_4O_2 + H \qquad \text{(R3)}$$

$$C_6H_5OO \leftrightarrow C_5H_5 + CO_2 \qquad \text{(R4)}$$

The rate coefficient of reaction R2 was calculated using QRRK analysis and the reverse rate constant by microscopic reversibility. Inclusion of reactions R3 and R4 was necessary, as will be shown below, to gain agreement between the predicted and experimental benzene concentration profile. However, reactions R3 and R4 are not elementary reactions, and rate coefficients for these overall steps were chosen so as to affect the radical pool to give the best fit between the mechanism predictions and the benzene concentration profile measured at 813 K, 246 bar, and residence times of 3–7 s. Their reverse rate coefficients were calculated by microscopic reversibility. Since the present rate coefficients for reactions R3 and R4 are semiempirical, any attempt to use them in other models should be pursued with caution. While the mechanisms by which reactions R3 and R4 take place have not been experimentally determined and likely involve never observed intermediates, theoretical calculations using density functional analysis show that reactions R3 and R4 involve one common isomerization path through a dioxetane cyclic intermediate. After this first isomerization, a path to $C_6H_4O_2 + H$ is present. A second series (unzipping process) is also present, along with another isomerization series. The rate-controlling step involves a 3,2,0 bicyclic (four plus five member ring) tight transition state. CO_2 results from the unimolecular decomposition of this bicyclic [35–37].

Justification for the inclusion of reaction R3 comes from the detection of $C_6H_4O_2$ during benzene combustion at both fuel-rich and fuel-lean conditions at 900–1300 K [25], our observation of $C_6H_4O_2$ in the oxidation of benzene under supercritical water conditions [16,19], and the incorporation of the overall reaction of C_6H_5 and O_2 to $C_6H_4O_2$ and H in the benzene combustion mechanism of Tan and Frank [24]. Since the reaction between C_6H_5 and O_2 predominantly forms C_6H_5OO at 246 bar and 813 K, reaction R3 was used in place of the addition/elimination reaction suggested by Frank et al. [33] to

account for $C_6H_4O_2$ production. Further reactions of $C_6H_4O_2$ were accounted for by incorporating a recent submechanism [38] by which $C_6H_4O_2$ is fully oxidized.

Reaction R4 is included to explain the very early appearance of CO_2 in benzene oxidation under supercritical water conditions [16]. The CO_2 yields exceeded those of CO at all conditions studied and for all conversions of benzene. Observations of CO_2 yields always exceeding those of CO were also reported in the SCWO of phenol [15,39] and substituted phenols [40–43], leading to speculation of pathways for CO_2 formation which do not involve CO. Additionally, in benzene combustion at 900–1300 K and at 350 Torr, Chai and Pfefferle [25] measured high amounts of CO_2 at low benzene conversions and postulated CO_2 production by routes other than the reaction of OH and CO. Carpenter [35], Barckholtz et al. [36] and our work [37] show that the reaction of C_6H_5 and O_2 leads to formation of C_5H_5 and CO_2. In the present study, since C_6H_5OO is the primary reaction product of C_6H_5 and O_2 at 246 bar and 813 K, reaction R4 was included in place of an addition/elimination reaction.

Comparison of Model Predictions and Measurements of Benzene Oxidation under Supercritical Water Conditions

The predictions of the benzene SCWO mechanism [16], developed by adapting the benzene combustion mechanism of Shandross et al. [17] and Shandross [18] for the present conditions (813 K, 246 bar, and fuel equivalence ratio, Φ, of 1.0), are compared in Fig. 1 (solid line) against the experimental data (points). Also shown is the profile predicted by the original mechanism of Shandross et al. [17] and Shandross [18] (long-dashed line), which generally represents the predictions of low-pressure benzene combustion mechanisms at SCWO conditions. Dissociation reactions of C_6H_5OO to $C_6H_4O_2$ and H and C_5H_5 and CO_2 were necessary in the SCWO mechanism to improve the agreement between the predictions and the data. With their inclusion, the shape and position of the predicted benzene concentration profile agree with the experimental data. The absolute values of the rate coefficients of reactions R3 and R4 were found not to have significant effects on the model predictions as long as the ratio of $k_{f,4}$ to $k_{f,3}$ is equal to 0.4. If this ratio is larger or smaller than 0.4, the predicted benzene reaction rate is too slow or too fast, respectively. Without inclusion of reaction R3 or R4, the predicted benzene oxidation rate is too fast and the reaction delay is too small (short-dashed line). The induction time can be varied from 0 to a maximum of ~1 s by changing the rate coefficient of reaction R3. The dashed-and-dotted line represents the
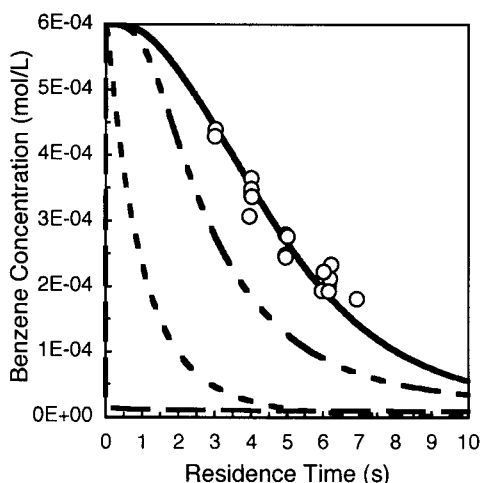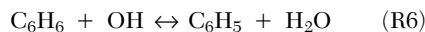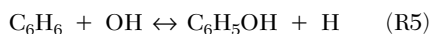

FIG. 1. Benzene concentration profiles predicted by the supercritical water benzene oxidation mechanism: $T = 813$ K; $P = 246$ bar; $\Phi = 1.0$; $[C_6H_6]_0 = 0.6 \times 10^{-3}$ mol/L; ($\bigcirc$) experimental data; — — mechanism of Shandross et al. [17] and Shandross [18]; ——— SCWO mechanism including reaction R3 $C_6H_5OO \leftrightarrow C_6H_4O_2 + H$ with $k_{f,3} = 4.0 \times 10^8$ s^{-1} and reaction R4 $C_6H_5OO \leftrightarrow C_5H_5 + CO_2$ with $k_{f,4} = 1.6 \times 10^8$ s^{-1}; ------ SCWO mechanism without reaction R3 or R4; —·—·— SCWO mechanism including only reaction R3 with $k_{f,3} = 4.0 \times 10^8$ s^{-1}.

slowest benzene oxidation rate that can be achieved through adjustment of $k_{f,3}$ (without including reaction R4).

The net rates of formation or destruction of key species by the individual reactions in the mechanism were calculated to determine the controlling reactions at 813 K and 246 bar with stoichiometric oxygen. By comparing the net rates of all reactions involving a single species, the primary destruction and formation pathways were determined.

Benzene was found to react almost exclusively by reactions R5 and R6:

$$C_6H_6 + OH \leftrightarrow C_6H_5OH + H \qquad \text{(R5)}$$

$$C_6H_6 + OH \leftrightarrow C_6H_5 + H_2O \qquad \text{(R6)}$$

with reaction R6 accounting for over 97% of the oxidation rate of benzene at 813 K and 246 bar. The rate coefficient used for reaction R6 [32] is the same as that used by Shandross et al. [17] and Shandross [18]. Although reaction R5 is recognized to proceed by a chemically activated pathway [44], given the relative unimportance of reaction R5 the rate coefficient used [45] is the same as that used by Shandross et al. [17] and Shandross [18]. The destruction of phenyl radical (C_6H_5) formed by reaction R6 is completely accounted for by reaction R7:
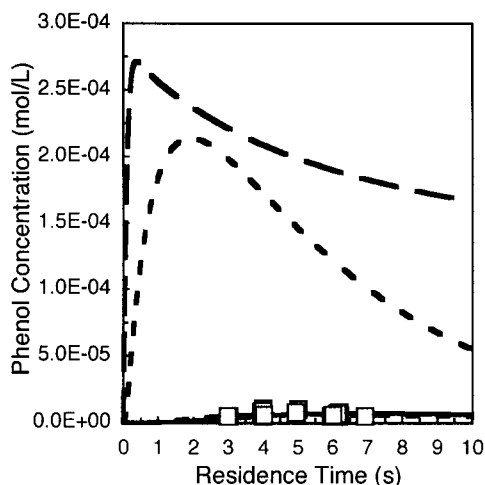
FIG. 2. Phenol concentration profiles predicted by the supercritical water benzene oxidation mechanism: $T = 813$ K; $P = 246$ bar: $\Phi = 1.0$; $[C_6H_6]_0 = 0.6 \times 10^{-3}$ mol/L; ($\square$) experimental data; — — mechanism of Shandross et al. [17] and Shandross [18]; ——— SCWO mechanism including reaction R3 $C_6H_5OO \leftrightarrow C_6H_4O_2 + H$ with $k_{f,3}$ 4.0×10^8 s^{-1} and reaction R4 $C_6H_5OO \leftrightarrow C_5H_5 + CO_2$ with $k_{f,4} = 1.6 \times 10^8$ s^{-1}; ------ SCWO mechanism without reaction R3 or R4; ----- (almost hidden by ———) SCWO mechanism including only reaction R3 with $k_{f,3} = 4.0 \times 10^8$ s^{-1}.

$$C_6H_5 + O_2 \leftrightarrow C_6H_5OO \qquad (R7)$$
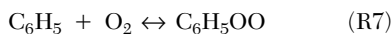
The fate of C_6H_5OO is the most critical unknown. Comparisons with the data suggest that the radical-forming, chain-branching loss channel to C_6H_5O and O (reaction R2) can only be a minor channel, and analysis of thermochemistry and the kinetics from the density functional analysis supports the ratio of 0.4 for $k_{f,4}/k_{f,3}$ under SCWO conditions [37].

The reactions and associated rate constants of cyclopentadienyl (C_5H_5) and cyclopentadiene (C_5H_6) in the Shandross mechanism were taken from the mechanism of Emdee et al. [21], in which the C_5H_5 submechanism was based on the outline presented by Brezinsky [46], and the abstraction of H from C_5H_6 by HO_2, OH, H, and O was estimated from the analogous reactions with formaldehyde. In the SCWO-mechanism, we computed rate coefficients using CHEMDIS for the addition and combination reactions of C_5H_5 and C_5H_6 at 246 bar from 300 to 1000 K using the data presented in Zhong and Bozzelli [47,48]. Reactions with the highest rate coefficients at 813 K and 246 bar were included in the benzene SCWO mechanism, according to which C_5H_5 from reaction R4 reacts primarily by reaction R8:
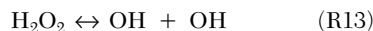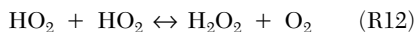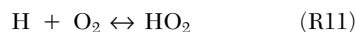
$$C_5H_5 + HO_2 \leftrightarrow C_5H_5O + OH \qquad (R8)$$

C_5H_5O then undergoes ring-opening reactions, leading eventually to CO and CO_2.

Since the oxidation of benzene proceeds mainly by reaction R6, the reaction delay (or induction time) and the subsequent rate of benzene reaction are determined by the rate of OH radical generation, which, in the present mechanism, is primarily by reaction R8.

If the global reactions R3 and R4 are not incorporated into the mechanism, reaction R2 is the dominant C_6H_5OO destruction channel. With O formed by reaction R2, excess OH is generated directly by reaction R9

$$O + H_2O \leftrightarrow OH + OH \qquad (R9)$$
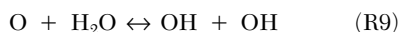
and indirectly by the following series of reactions:

$$C_6H_6 + O \leftrightarrow C_6H_5O + H \qquad (R10)$$

$$H + O_2 \leftrightarrow HO_2 \qquad (R11)$$

$$HO_2 + HO_2 \leftrightarrow H_2O_2 + O_2 \qquad (R12)$$

$$H_2O_2 \leftrightarrow OH + OH \qquad (R13)$$

Reaction R6 proceeds much too quickly, and the present mechanism overpredicts the benzene oxidation rate.

As stated previously, the rate coefficients of reactions R3 and R4 were chosen to optimize model-data agreement for the benzene concentration profile. Including reaction R3 with a higher rate constant than reaction R2 eliminates the rapid formation of O and the subsequent overproduction of OH by reaction R9. Since reaction R3 generates H, OH formation proceeds through reactions R11, R12, and R13, and inclusion of reaction R3 alone cannot decrease the rate of benzene oxidation sufficiently to bring the model into agreement with the data. As discussed earlier, the reaction of H and O_2 producing OH and O is not important at SCWO conditions. To gain model-data agreement, reaction R4 was included. The inclusion of reaction R4 slows the benzene oxidation rate, as C_5H_5 is relatively unreactive. Reaction R4 also provides a pathway for CO_2 formation to account for the experimental observation that CO_2 yields exceed those of CO for all measured residence times and reaction conditions [19]. Without reaction R4, the model incorrectly predicts that the CO_2 concentration remains below that of CO for residence times less than 7 s. Even with reaction R4, the model underpredicts the concentrations of CO and CO_2, reflecting inadequate chemistry for further oxidation of intermediate species. A large fraction of carbon remains as $C_6H_4O_2$, and $C_6H_3O_2$, C_5H_5O, C_4H_4, and H_2CCCCH are also significant.

Figure 2 demonstrates that with inclusion of reactions R3 and R4, the predicted C_6H_5OH concentration profile agrees with the experimental data.
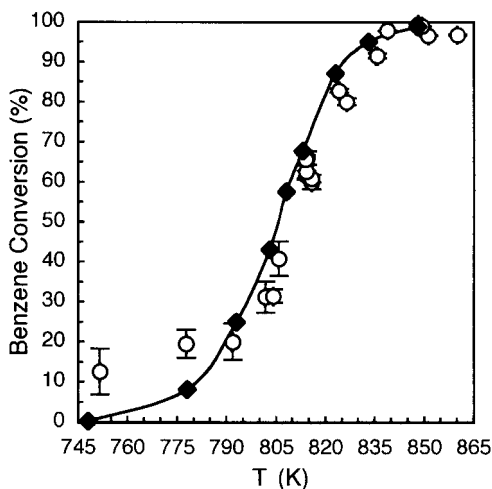
FIG. 3. Comparison of predicted (—◆—) and measured (○) benzene conversions at various temperatures: $\tau = 6.2$ s; $P = 246$ bar; $\Phi = 1.0$; $[C_6H_6]_0 = 0.6 \times 10^{-3}$ mol/L.
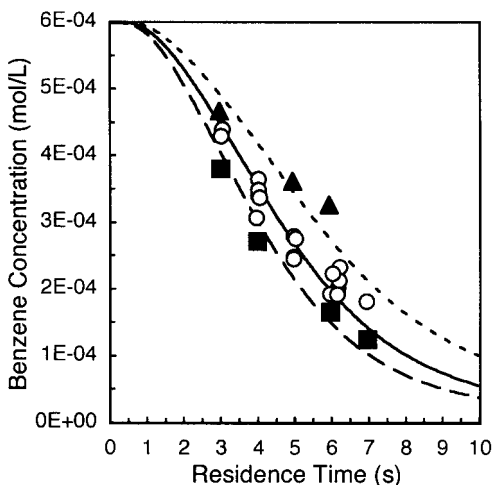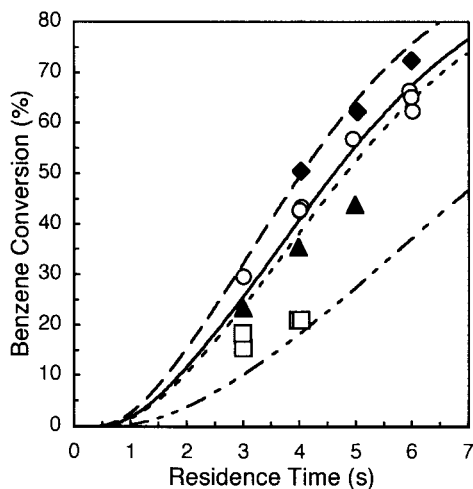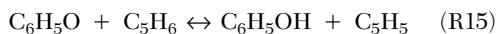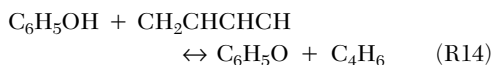

FIG. 5. Comparison of predicted (lines) and measured (symbols) benzene conversions at four water densities: (◆, – –) $\rho = 0.091$ g/mL ($P = 278$ bar); (○, ——) $\rho = 0.079$ g/mL ($P = 246$ bar); (▲, - - - - -) $\rho = 0.072$ g/mL ($P = 228$ bar); (□, —-—-) $\rho = 0.041$ g/mL ($P = 139$ bar). $T = 813$ K; $[C_6H_6]_0 = 0.6 \times 10^{-3}$ mol/L; $\Phi = 1.0$.

FIG. 4. Comparison of predicted (lines) and measured (symbols) benzene concentrations at three fuel equivalence ratios (Φ): (■, – –) $\Phi = 0.5$; (○, ——) $\Phi = 1.0$; (▲, - - - -) $\Phi = 2.5$. $T = 813$ K; $P = 246$ bar; $[C_6H_6]_0 = 0.6 \times 10^{-3}$ mol/L.

Without reactions R3 and R4, phenol is overpredicted by a factor of ~100. Phenol is initially formed by reaction R5, destroyed by reaction R14, and then reformed in reaction R15 in an equimolar exchange:

$$C_6H_5OH + CH_2CHCHCH \leftrightarrow C_6H_5O + C_4H_6 \quad (R14)$$

$$C_6H_5O + C_5H_6 \leftrightarrow C_6H_5OH + C_5H_5 \quad (R15)$$

Rate coefficients for reactions R14 and R15 were kept at the values used by Shandross et al. [17] and Shandross [8]. Given that reactions R14 and R15 are the principal reactions involving both C_6H_5O and C_6H_5OH and that C_6H_5OH is minor compared with C_6H_5 as a benzene decomposition product, C_6H_5O is also not a key intermediate in the SCWO mechanism. Without reaction R3, excess C_6H_5O is formed by reaction R2, leading to the overprediction of C_6H_5OH. With all reactions which lead to C_6H_5OH formation in the SCWO mechanism involving C_6H_5O with the exception of reaction R5, and given that reaction R5 is not competitive with reaction R6 at these conditions, agreement between the experimental and predicted C_6H_5OH concentrations indicates that C_6H_5O concentration is now properly predicted as long as the C_6H_5O/C_6H_5OH chemistry is correctly represented.

To test the robustness of the mechanism, the model predictions were compared with benzene SCWO measurements over considerable ranges of reactor conditions [19]. No further adjustments were made to the mechanism. The rate constants of reactions R3 and R4 were treated as temperature independent. Benzene concentrations predicted by the model as a function of temperature at a given pressure, equivalence ratio, and residence time are compared with the experimental data in Fig. 3. Predicted benzene concentration profiles are compared with the data at equivalence ratios from 0.5 to 2.5 at a given temperature and pressure in Fig. 4 and over a range of water densities or pressures at a given

temperature and equivalence ratio in Fig. 5. The good agreement seen between predictions and experimental data in all cases is especially encouraging in view of the ranges of conditions covered.

Summary and Conclusions

A benzene SCWO mechanism was developed using published benzene combustion mechanisms and submechanisms describing the oxidation of key intermediates. To adapt the benzene combustion mechanism to the lower temperatures and higher pressures of SCWO, new reaction pathways were added and QRRK theory was used to calculate the rate coefficients and predict reaction products for pressure-dependent reactions. The most important difference between the benzene oxidation mechanism for supercritical water conditions and those for combustion conditions is reactions in supercritical water involving C_6H_5OO predicted to be formed by C_6H_5 reacting with O_2. By adjusting the rate constants of two proposed, global thermal decomposition reactions of C_6H_5OO, the first forming p-benzoquinone and H and the second forming cyclopentadienyl and CO_2, the model was fit to the benzene concentration profile measured during SCWO at 813 K, 246 bar, and 3–7 s residence time with stoichiometric oxygen. The resulting mechanism accurately reproduces the experimental benzene and phenol concentration profiles at these conditions and predicts well the benzene concentration profiles under SCWO conditions ranging from 750 to 850 K, 139 to 278 bar, and equivalence ratios from 0.5 to 2.5.

REFERENCES

1. Killilea, W. R., and Swallow, K. C., *J. Supercrit. Fluids* 5:72 (1992).

2. Holgate, H. R., and Tester, J. W., *Combust. Sci. Technol.* 88:369 (1993).

3. Holgate, H. R., and Tester, J. W., *J. Phys. Chem.* 98:810 (1994).

4. Paterson, C., Breshears, D., and Foy, B., *Combust. Sci. Technol.* 89:411 (1993).

5. Dagaut, P., Daney de Marcillac, B., Tan, Y., Cathonnet, M., and Boettner, J.-C., *J. Chim. Phys.* 92:1124 (1995).

6. Brock, E. E., and Savage, P. E., *AIChE J.* 41:1874 (1995).

7. Alkam, M. K., Pai, V. M., Butler, P. B., and Pitz, W. J., *Combust. Flame* 106:110 (1996).

8. Webley, P. A., and Tester, J. W., *Energy Fuels* 5:411 (1991).

9. Savage, P. E., Yu, J. L., Stylski, N., and Brock, E. E., *J. Supercrit. Fluids* 12:141 (1998).

10. Webley, P. A., and Tester, J. W., in *Supercritical Fluid Science and Technology* (K. P. Johnston and J. M. L. Penninger, eds.), ACS Symposium Series 406, American Chemical Society, Washington, DC, 1989, p. 259.

11. Butler, P. B., Bergan, N. E., Bramlette, T. T., Pitz, W. J., and Westbrook, C. K., *Oxidation of Hazardous Waste in Supercritical Water: A Comparison of Modeling and Experimental Results for Methanol Destruction,* U.S. Department of Energy report DE91-017097, 1991.

12. Schmitt, R. G., Butler, P. B., Westbrook, C. K., and Pitz, W. J., *Destruction of Hazardous Waste in Supercritical Water, Part II: A Study of High Pressure Methanol Oxidation Kinetics,* U.S. Department of Energy report DE92-008559, 1991.

13. Butler, P. B., Bergan, N. E., Bramlette, T. T., Westbrook, C. K., and Pitz, W. J., "*Oxidation of Hazardous Waste in Supercritical Water, Part I: A Comparison of Modeling and Experimental Results for Methanol Destruction,*" U.S. Department of Energy report DE92-008565, 1991.

14. Dagaut, P., Cathonnet, M., and Boettner, J.-C., *J. Supercrit. Fluids* 9:33 (1996).

15. Gopalan, S., and Savage, P. E., in *Innovations in Supercritical Fluids* (K. W. Hutchenson and N. R. Foster, eds.), ACS Symposium Series 608, American Chemical Society, Washington, DC, 1995, p. 217.

16. DiNaro, J. L., Ph.D. thesis, "Oxidation of Benzene in Supercritical Water: Experimental Measurements and Development of an Elementary Reaction Mechanism," Department of Chemical Engineering, Massachusetts Institute of Technology, Cambridge, MA, 1999.

17. Shandross, R. A., Longwell, J. P., and Howard, J. B., *Proc. Combust. Inst.* 26:711 (1996).

18. Shandross, R. A., Ph.D. thesis, "Expermental and Theoretical Study of Hydrogen and Benzene Destruction Chemistries," Department of Chemical Engineering, Massachusetts Institute of Technology, Cambridge, MA, 1996.

19. DiNaro, J. L., Tester, J. W., Swallow, K. C., and Howard, J. B., *AIChE J.* (2000).

20. Bittker, D. A., *Combust. Sci. Technol.* 79:49 (1991).

21. Emdee, J. L., Brezinsky, K., and Glassman, I., *J. Phys. Chem.* 96:2151 (1992).

22. Lindstedt, R. P., and Skevis, G., *Combust. Flame* 99:551 (1994).

23. Zhang, H.-Y., and McKinnon, J. T., *Combust. Sci. Technol.* 107:261 (1995).

24. Tan, Y., and Frank, P., *Proc. Combust. Inst.* 26:677 (1996).

25. Chai, Y., and Pfefferle, L. D., *Fuel* 77:313 (1998).

26. Dean, A. M., *J. Phys. Chem.* 89:4600 (1985).

27. Dean, A. M., Bozzelli, J. W., and Ritter, E. R., *Combust. Sci. Technol.* 80:63 (1991).

28. Ing, W.-C., Ph.D. thesis, Department of Chemical Engineering, New Jersey Institute of Technology, Newark, NJ, 1995.

29. Chang, A. Y., Bozzelli, J. W., and Dean, A. M., *Zeitschrift für Physikalische Chemie* (2000).

30. Westmoreland, P. R., Howard, J. B., Longwell, J. P., and Dean, A. M., *AIChE J.* 32:1971 (1986).

31. Cobos, C. J., Hippler, H., and Troe, J., *J. Phys. Chem.* 89:342 (1985).

32. Baulch, D. L., Cobos, C. J., Cox, R. A., Esser, C., Frank, P., Just, T., Kerr, J. A., Pilling, M. J., Troe, J., Walker, R. W., and Warnatz, J., *J. Phys. Chem. Ref. Data* 21:411 (1992).

33. Frank, P., Herzler, J., Just, T., and Wahl, C., *Proc. Combust. Inst.* 25 (1994).

34. Yu, T., and Lin, M. C., *J. Am. Chem. Soc.* 116:9571 (1994).

35. Carpenter, B. K., *J. Am. Chem. Soc.* 115:9806 (1993).

36. Barckholtz, C., Fadden, M. J., and Hadad, C. M., *J. Phys. Chem.* 103:8108 (1999).

37. Sebbar N., Bockhorn, H., and Bozzelli, J. W., 28th Symposium (International) on Combustion, The Combustion Institute (2000) [Abstract only].

38. Alzueta, M. U., Oliva, M., and Glarborg, P., *Int. J. Chem. Kin.* 30:683 (1998).

39. Krajnc, M., and Levec, J., *AIChE J.* 42:1977 (1996).

40. Martino, C. J., Savage, P. E., and Kasiborski, J., *Ind. Eng. Chem. Res.* 34:1941 (1995).

41. Martino, C. J., and Savage, P. E., *Ind. Eng. Chem. Res.* 36:1391 (1997).

42. Martino, C. J., and Savage, P. E., *Ind. Eng. Chem. Res.* 38:1784 (1999).

43. Martino, C. J., and Savage, P. E., *Ind. Eng. Chem. Res.* 38:1775 (1999).

44. Lay, T. S., Bozzelli, J. W., and Seinfeld, J. H., *J. Phys. Chem.* 100:6543 (1996).

45. He, Y. Z., Mallard, W. G., and Tsang, W., *J. Phys. Chem.* 92:2196 (1988).

46. Brezinsky, K., *Prog. Energy Combust. Sci.* 12:1 (1986).

47. Zhong, X., and Bozzelli, J. W., *Int. J. Chem. Kin.* 29:893 (1997).

48. Zhong, X., and Bozzelli, J. W., *J. Phys. Chem.* 102:3537 (1998).

COMMENTS

Alexander Fridman, University of Illinois at Chicago, USA. Standard mechanisms of C_6H_6 oxidation in gas phase cannot be used for oxidation in supercritical water. When looking for special new oxidation channels in supercritical water, it would probably be important to take into consideration ion formation and following ion-molecular reactions like $H_3O^+ + H_2O \rightarrow H_4O^+ + OH$, and so on, leading to OH formation. Such reactions in supercritical conditions can be important when working at higher temperature limits.

Author's Reply. Ionic reactions were not considered because the supercritical water environment at our conditions (475–600 C, 250 bar) does not support ionic species due to the low dielectric constant of water. In addition, typical ionization potentials are 200 kcal/mol, whereas bond energies are about 100 kcal/mol.

•

Horst Hippler, University of Karlsruhe, Germany. There is an alternative mechanism for the oxidation of benzene from atmospheric chemistry. OH radicals add to the benzene $OH + C_6H_6 \rightleftharpoons C_6H_6OH$ (pre-equilibrium) and then C_6H_6OH reacts with O_2. Could this be an alternative start into the SCWO of benzene? Additionally, the oxidation of CO with OH is strongly pressure dependent. The rate constant increases strongly with increasing pressure. Could this account for preferential finding CO_2 and not CO?

Author's Reply. The addition of OH to benzene to form a cyclohexadienyl-OH adduct followed by reaction with O_2 is important in atmospheric chemistry (Lay et al., 1997), but not very important in combustion. The lifetime for dissociation of the cyclohexadienyl-OH adduct back to OH + benzene is not the order of 1 s at atmospheric temperature, but only about 3 μs at SCWO temperatures. A more important reaction of the cyclohexadienyl-OH adduct at SCWO conditions is H-atom elimination to phenol + H. Here, reverse dissociation to benzene + OH is favored because of the higher entropy of OH + benzene relative to H + phenol and a slightly lower (less than 2 kcal/mol) lower enthalpy for the dissociation. This reaction was taken into account by including the high pressure value of He et al. (1988) for the overall reaction.

The reaction of CO and OH proceeds through the formation of an activated HOCO intermediate. At high pressures, the stabilization pathway to HOCO dominates over the dissociation pathway to CO_2 + H (Fulle et al., 1996). Stabilized HOCO can then undergo reaction, including dissociation back to CO + OH or to CO_2 + H. As is the case with the cyclohexadienyl-OH adduct, reverse dissociation to products is favored over the CO_2 + H pathway.